The three-dimensional structure of Ca^{2+}-bound calcyclin: implications for Ca^{2+}-signal transduction by S100 proteins

Mallika Sastry[1], Randal R Ketchem[1], Orlando Crescenzi[1], Christoph Weber[1], Michael J Lubienski[1], Hiroyoshi Hidaka[2] and Walter J Chazin[1]*

Background: Calcyclin is a member of the S100 subfamily of EF-hand Ca^{2+}-binding proteins. This protein has implied roles in the regulation of cell growth and division, exhibits deregulated expression in association with cell transformation, and is found in high abundance in certain breast cancer cell lines. The novel homodimeric structural motif first identified for apo calcyclin raised the possibility that S100 proteins recognize their targets in a manner that is distinctly different from that of the prototypical EF-hand Ca^{2+} sensor, calmodulin. The NMR solution structure of Ca^{2+}-bound calcyclin has been determined in order to identify Ca^{2+}-induced structural changes and to obtain insights into the mechanism of Ca^{2+}-triggered target protein recognition.

Results: The three-dimensional structure of Ca^{2+}-bound calcyclin was calculated with 1372 experimental constraints, and is represented by an ensemble of 20 structures that have a backbone root mean square deviation of 1.9 Å for the eight helices. Ca^{2+}-bound calcyclin has the same symmetric homodimeric fold as observed for the apo protein. The helical packing within the globular domains and the subunit interface also change little upon Ca^{2+} binding. A distinct homology was found between the Ca^{2+}-bound states of the calcyclin subunit and the monomeric S100 protein calbindin D_{9k}.

Conclusions: Only very modest Ca^{2+}-induced changes are observed in the structure of calcyclin, in sharp contrast to the domain-opening that occurs in calmodulin and related Ca^{2+}-sensor proteins. Thus, calcyclin, and by inference other members of the S100 family, must have a different mode for transducing Ca^{2+} signals and recognizing target proteins. This proposal raises significant questions concerning the purported roles of S100 proteins as Ca^{2+} sensors.

Addresses: [1]Department of Molecular Biology (MB-9), The Scripps Research Institute, 10550 North Torrey Pines Road, La Jolla, California 92037, USA and [2]Department of Pharmacology, Nagoya University Medical School, Nagoya 466, Japan.

*Corresponding author.
E-mail: chazin@scripps.edu

Key words: calcium-binding protein, calcium signaling, conformational change, NMR, signal transduction

Received: **27 October 1997**
Revisions requested: **24 November 1997**
Revisions received: **18 December 1997**
Accepted: **6 January 1998**

Structure 15 February 1998, **6**:223–231
http://biomednet.com/elecref/0969212600600223

Introduction

The Ca^{2+} ion serves as a second messenger in numerous signal transduction pathways that control a wide range of cellular processes from cell-cycle progression to metabolic control. The readout of calcium signals is frequently mediated by a member of the EF-hand family of Ca^{2+}-binding proteins (CaBPs). The prototypical EF-hand Ca^{2+} sensor is calmodulin, and structural analysis by nuclear magnetic resonance (NMR) spectroscopy has defined the nature of the conformational changes which lead to its activation and subsequent binding to many intracellular targets [1–3]. A similar result has been obtained by NMR for another Ca^{2+} sensor, troponin C [4]. The Ca^{2+}-induced opening of the bilobed, globular EF-hand domain, which results in a considerable increase in hydrophobic accessible surface (the HMJ model) [5], has served as a paradigm for the Ca^{2+} signal transduction field. This mode of Ca^{2+} activation has been confirmed by three-dimensional structures of Ca^{2+}-activated calmodulin bound to peptide fragments of target proteins [6–8].

In 1995, the three-dimensional structure of calcyclin in the inactivated Ca^{2+}-free state was reported, revealing a novel homodimeric structural motif among the EF-hand CaBPs [9]. The fundamental differences between the packing of the EF-hand domains of calcyclin and calmodulin implied that calcyclin has a distinct mode of target recognition. Subsequent structure determination of the related protein S100β confirmed the generality of the calcyclin homodimer motif [10–11]. As these proteins are purported to transduce Ca^{2+} signals [12], but have structures that are inconsistent with the calmodulin paradigm, one is lead to question how the dimeric structure is triggered to interact with its receptor(s). Here we report a first step towards addressing this question, the determination of the three-dimensional structure of Ca^{2+}-bound calcyclin.

Calcyclin and S100β are members of the S100 subfamily of EF-hand CaBPs [12], which is characterized by N-terminal binding sites that are distinct from the EF-hand prototype. In these proteins, the N-terminal binding loops

are 14 residues in length, as opposed to 12, and chelation of the Ca^{2+} ion involves a different set of ligands to those normally used in EF-hand CaBPs. In the S100 proteins, in addition to the highly conserved bidentate glutamic acid sidechain carboxylate, four mainchain carbonyl oxygens are utilized to chelate the Ca^{2+} ion, as opposed to the three sidechain carbonyl oxygens and one mainchain oxygen used in prototypical EF-hands [13].

The purported functions of S100 proteins range from the regulation of cellular events to direct roles in Ca^{2+} transport [12]. Calcyclin has been implicated in the regulation of cell growth and proliferation because its messenger RNA is preferentially expressed in the G_1 phase of the cell cycle [14–16]. The genes for many of the S100 proteins are found to be clustered in a specific region on human chromosome 1q21, a site that is frequently rearranged in specific tumor tissues [17]. This, combined with the observation of deregulated expression of calcyclin and other S100 proteins in certain tumor tissues, suggests a role for these proteins in oncogenesis. For example, calcyclin expression is increased and deregulated in the cells of patients with acute myeloid leukemia [16–18], and the gene product is abundant in certain human breast cancer and melanoma cell lines [19]. At the functional level, calcyclin has been shown to bind Ca^{2+}/phospholipid-binding proteins of the annexin family, glyceraldehyde-3-phosphate dehydrogenase, and a 30 kDa protein present in Ehrlich ascites tumor cells [20–23]. A specific regulatory function for calcyclin in cell growth or division is suggested by its calcium-dependent binding to annexin XI (CAP-50) [20,24–26].

In this report we describe the three-dimensional solution structure of Ca^{2+}-bound calcyclin determined by NMR spectroscopy. The structure is then compared to the Ca^{2+}-bound state of the homologous S100 protein calbindin D_{9k}, as well as to the apo states of calcyclin, calbindin D_{9k} and S100β. Ca^{2+}-induced conformational changes in calcyclin are determined from the comparison of the structures in the absence and presence of calcium, and the implications of our findings are discussed in terms of the molecular basis for signal transduction by S100 proteins.

Results and discussion

Structure determination

The structure of recombinant rabbit lung calcyclin in the Ca^{2+}-bound state was determined in solution by a combination of homonuclear and heteronuclear NMR approaches [27]. As for the symmetric homodimeric apo state of the protein, a single set of ^1H resonance lines is observed. The line widths in the presence of Ca^{2+} are significantly larger than in its absence, suggesting that in addition to the specific dimerization, there is an increase in the tendency of the protein to associate at the ~1 mM concentrations required for NMR. This is a common observation among EF-hand CaBPs, and is typically associated with an increase in the exposed hydrophobic surface upon binding of Ca^{2+}. Backbone ^1H, ^{13}C and ^{15}N resonance assignments have been obtained for all but three residues (Ser3, Gly24 and Asn85). In addition, ~70% of the sidechain resonances were assigned, including all but two of the critical methyl and aromatic ring ^1H resonances. The elements of secondary structure and the global folding pattern of the monomer were determined after resonance assignment, according to previously published methods [27].

The three-dimensional structure of Ca^{2+}-bound calcyclin was calculated using the strategy developed for apo calcyclin, with an initial stage of distance geometry and restrained molecular dynamics (rMD) on the monomer subunit, followed by docking of two copies of the monomer and additional rMD refinement [9,28]. The calculations were performed in an iterative manner, continually revising and increasing the input nuclear Overhauser effect (NOE) distance constraint list. The initial family of structures was calculated using only unambiguously identified NOEs. This family was then used to calculate the mean distances (and standard deviations) corresponding to all possible NOE cross-peak assignments. Additional cross-peaks were assigned for those cases where only a single option fell below a very conservatively set upper limit (10 Å for most rounds). This process was repeated until there were no further changes in the constraint list. The final set of input data for the dimer included 1088 (544×2) distance restraints derived from the two-dimensional and three-dimensional NOE (NOESY) spectra: 380 intraresidue, 240 sequential, 278 medium range, 106 long range and 84 intersubunit. An additional 80 (40×2) distance restraints for 40 hydrogen bonds, and 204 (102×2) backbone dihedral angle restraints were included in the calculation, bringing the total to 1372. All of the 60 distance geometry starting structures were successfully embedded. Of these, 27 were successfully minimized and refined by rMD. The four best monomers were used for rMD docking to create 192 dimer structures, of which 56 converged to the final dimer fold. Analysis of the ensemble showed that a minimum of 20 structures was required to represent the conformational space consistent with the experimental data. The selection of these structures is described in the Materials and methods section.

The representative ensemble of 20 converged structures had only small violations and low molecular energies. Structural statistics are provided in Table 1. It is important to note that symmetry restraints were not imposed during any phase of the structure calculations, yet the pairwise root mean square deviation (rmsd) between the mean subunit structures is low, reflecting the expected symmetry between the two subunits. The helices comprise the most well-defined regions of the structure and exhibit a

Table 1

Structural statistics for the ensemble of Ca^{2+}-bound calcyclin structures.

Constraint violations (mean and standard deviation)	
number of distance constraint violations ≥ 0.2 Å	0.2 ± 0.4
number of dihedral angle constraint violations ≥ 5°	1.0 ± 0.7
per structure maximum distance constraint violation (Å)	0.2 ± 0.0
per structure maximum dihedral constraint violation (°)	5.9 ± 1.4
AMBER energies (kcal mol^{-1}) (mean and standard deviation)	
constraint energy	7.4 ± 0.7
total energy	−2725 ± 24
Root mean square deviation (rmsd) from mean dimer structure (Å)	
residues in helices* (backbone /all heavy atom)	1.9 ± 0.4 / 2.4 ± 0.3
all residues (backbone /all heavy atom)	2.7 ± 0.3 / 3.3 ± 0.3
Rmsd between mean subunit† A and mean subunit B (Å)	
residues in helices* (backbone /all heavy atom)	0.3 / 0.3
all residues (backbone /all heavy atom)	0.4 / 0.5

*Helices are defined as: I, residues 5–20; II, 30–41; III, 50–61; and IV, 70–84. †Mean subunit structure calculated from the ensemble of 20 (Ca^{2+}-bound) dimer structures.

backbone rmsd from the mean of 1.9 Å after fitting over all eight helices. The precision of the subunit structure was better than the dimer, with an average rmsd from the mean of 1.5 Å for the helix backbones. Thus, the relative orientation of the two subunits was not as well determined as the subunits themselves. Furthermore, the relative orientation of helix III is poorly defined at the current level of analysis because there are only a few distance restraints to the rest of the protein. Although the identity of the Ca^{2+}-binding ligands in calcyclin can be established on the basis of sequence homology with the EF-hand CaBP family, no ions were included in the calculations. The absence of ions contributes to the coordinate uncertainty in the binding loops [29], in particular in the N-terminal half of the binding loops, which are found to be poorly defined. The N and C termini, along with the linker loop between the two EF-hands are also poorly defined; ^{15}N relaxation experiments (OC and WJC, unpublished results) indicate that this effect is due to enhanced motional flexibility in these three regions, as observed in other EF-hand CaBPs.

Description of the structure and comparison to apo calcyclin and other S100 proteins

Two views of the Ca^{2+}-bound calcyclin homodimer are shown in Figure 1. The structure of each subunit is comprised of a globular domain containing a pair of helix-binding loop-helix (EF-hand) motifs that are joined by an ill-defined linker loop. The EF-hands are packed in a parallel fashion, with a short, antiparallel β-type interaction between the two binding loops. This is similar to the arrangement seen in the globular domains of other EF-hand CaBPs [30]. The distribution of the elements of secondary structure, and in fact the three-dimensional structures of the EF-hand domains, are found to be very similar to those of apo calcyclin, apo S100β [10–11], and calbindin D_{9k} in both the apo and Ca^{2+}-bound states [31]. The structures of these EF-hand domains are also very similar to the closed conformation of the prototypical Ca^{2+} sensor calmodulin in the absence of Ca^{2+}, but clearly different from the open conformation of the Ca^{2+}-bound protein [32]. The only significant difference between the various calcyclin, calbindin D_{9k} and S100β structures is the

Figure 1

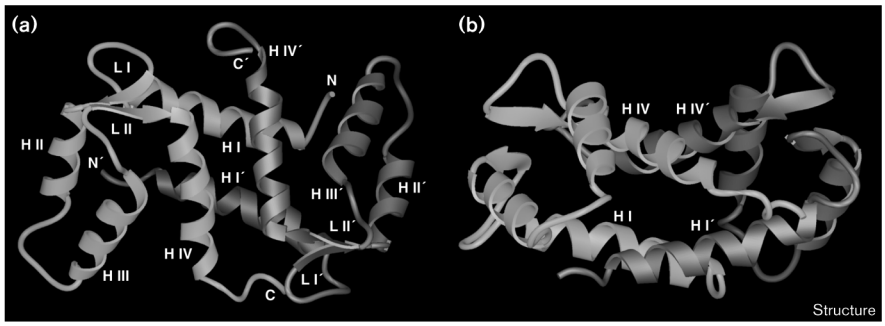

The three-dimensional structure of Ca^{2+}-bound calcyclin. **(a)** Ribbon drawing showing the antiparallel packing of the two subunits (depicted in salmon and blue) and the close contact between helices IV and IV′. The structural elements (H, helix; L, Ca^{2+}-binding loop) are labeled consecutively from the N termini. **(b)** The same ribbon drawing rotated by 90° (x) and 45° (y) to show a complementary view accentuating the helical packing; the figure is labeled as in (a). (Figure prepared using the Ribbons program [46] ported to the AVS software environment [AVS Inc.] by A Shah.)

Figure 2

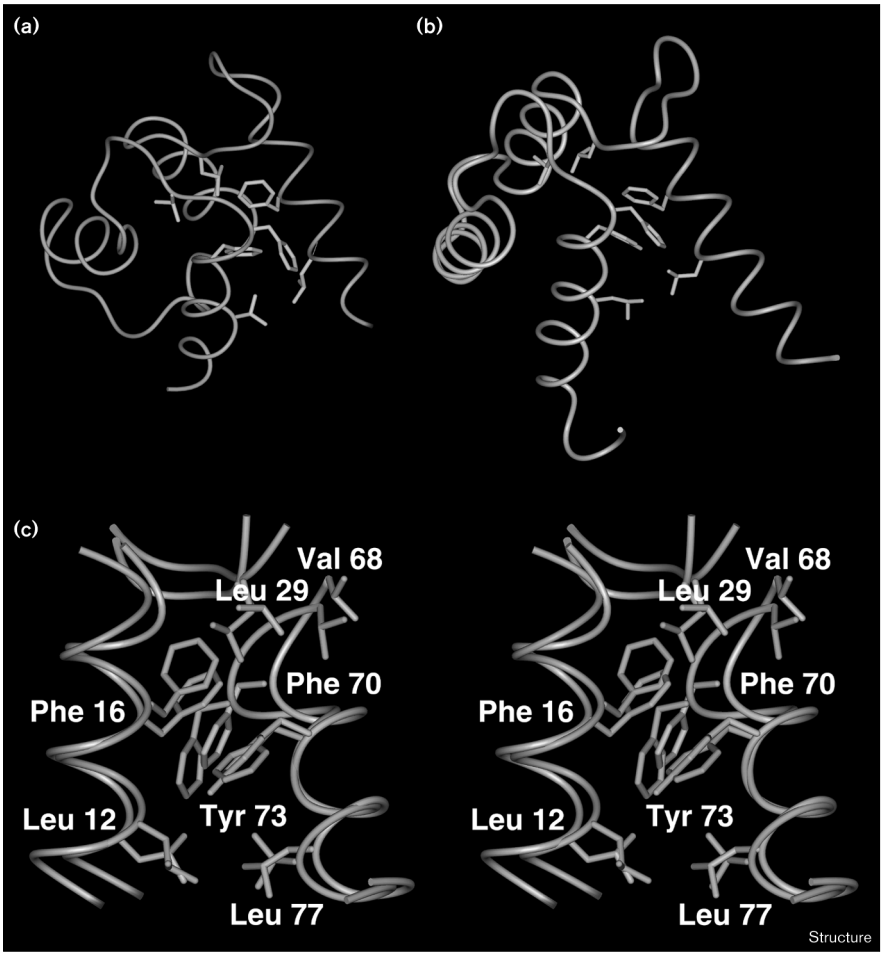

Comparison of the three-dimensional structures of calcyclin and calbindin D_{9k} in the Ca^{2+}-bound state. Overview of calbindin D_{9k} **(a)** and the calcyclin subunit **(b)**, highlighting the conserved residues in the hydrophobic core (cyan). The two structures were first overlaid by best-fit superposition of the backbone atoms of helices I, II and IV, then separated for viewing. **(c)** Stereo close-up view of the conserved hydrophobic residues at the interface between helices I and IV, showing the similarity in the packing of corresponding sidechains. The structures were overlaid by best-fit superposition of the backbone atoms of helices I and IV. Calbindin D_{9k} is shown in yellow and calcyclin is in salmon; the sidechains are labeled for calcyclin only. The coordinates for calbindin D_{9k} were obtained from the Brookhaven PDB (accession code 2BCB). (Figure prepared using Insight II [Version 95.0; MSI, San Diego].)

unique position of helix III in apo rat S100β [11]. This difference is very small, however, relative to the Ca^{2+}-induced structural changes observed in calmodulin.

The very high level of homology between the three-dimensional structure of the calcyclin dimer subunit and calbindin D_{9k}, first noted in the apo states [28], is retained in the Ca^{2+}-bound state (Figure 2). The interhelical angles for the apo and Ca^{2+}-bound states of both proteins are reported in Table 2, along with the values for apo rat S100β for comparison. The homology between calcyclin and calbindin D_{9k} extends to the sidechains that are important for maintaining the packing of the hydrophobic core. Seven residues (Leu12, Phe16, Leu29, Val68, Phe70, Tyr73 and Leu77 in calcyclin) are identical to those in calbindin D_{9k} or conservatively substituted, and each of these is found to pack in a highly similar manner (Figure 2c).

A series of comparisons of the apo and Ca^{2+}-bound state of calcyclin have been made. Statistically significant structural changes are observed upon binding of Ca^{2+} (rmsd from the mean for the eight helices is 5.3 Å), but overall these changes are modest (Figure 3a). Fitting-independent methods, including distance difference matrix and inter-residue contact analysis (as discussed elsewhere [32]), were utilized to ensure that the analysis was not biased by the selection of atoms for superposition. As these are not high-resolution structures, great care was taken in these studies to ensure that conclusions were drawn only where clearly warranted. The current analysis is somewhat limited by the relatively high uncertainties, particularly in the N terminus of helix I and in the packing of helix III in the apo protein. In addition, the relative orientation of the two subunits is not as well defined as the subunits themselves due to the difficulties of identifying NOEs at the subunit interface. Consequently, the similarity evident from superposition of the monomer subunit is even higher than from comparisons at the level of the dimer (Figures 3a and 3b; Table 3).

The dimer interface is mediated primarily by hydrophobic sidechain–sidechain interactions, as observed previously for apo calcyclin and apo S100β. Helices IV and IV′ form a

Table 2

Interhelical angles for calcyclin, calbindin D_{9k} and S100β*.

Helices†	Calcyclin–Ca^{2+}	Calbindin–Ca^{2+}	Apo calcyclin	Apo S100β	Apo calbindin
I–II	110 ± 8	128 ± 2	128 ± 11	135 ± 3	119 ± 3
I–III	−81 ± 16	−114 ± 6	−84 ± 18	−24 ± 2	−113 ± 3
I–IV	126 ± 5	125 ± 5	118 ± 13	121 ± 2	124 ± 3
II–III	161 ± 10	111 ± 5	147 ± 12	−138 ± 4	123 ± 6
II–IV	−36 ± 13	−33 ± 4	−23 ± 8	−36 ± 2	−36 ± 5
III–IV	135 ± 12	120 ± 7	147 ± 13	−142 ± 2	121 ± 7
IV–IV′	149 ± 4	–	148 ± 6	161 ± 2	–

*Interhelical angles were calculated using software written by SM Gagné (University of Alberta, Edmonton). †The helices in calcyclin, calbindin D_{9k} and S100β are designated: I (5–20, 3–14, 2–18); II, (30–41, 24–35, 29–40); III, (50–61, 46–54, 50–62); and IV, (70–83, 63–74, 70–82), respectively. The coordinates for apo calcyclin (1CNP), calbindin D_{9k} (2BCB, Ca^{2+}-bound; 1CLB, apo) and rat apo S100β (1SYM) were obtained from the Brookhaven PDB.

large portion of the dimer interface in both the apo and Ca^{2+}-bound calcyclin structures, but additional I–I′ and I–IV′ intersubunit contacts are present in the Ca^{2+}-bound structure. The ability to identify these additional contacts is not the result of an intrinsic difference between the apo and Ca^{2+}-bound calcyclin, but rather is due to the inclusion of heteronuclear NMR data for the Ca^{2+}-bound protein. Similar contacts were reported for apo S100β [10–11], and appear to be present in apo calcyclin based on our subsequent analysis of heteronuclear NMR experiments (L Mäler and WJC, unpublished results). The helix IV–IV′ angle for Ca^{2+}-bound calcyclin is 149 ± 4° similar to the value of 148 ± 6° in the apo state, and packing at the IV–IV′ interface is very similar in the presence and absence of Ca^{2+} (Figure 3c). The sidechains of residues contributing to the integral network of hydrophobic interactions at each end of the dimer interface are also packed in a very similar manner in the apo and Ca^{2+}-bound states. A close-up view of four of the five residues previously identified as appearing to be critical to the dimer interface (Ile13, Phe16, Phe70 and Leu88) is shown in Figure 3d. All these residues remain much less accessible to solvent in the dimer than they would be in an isolated subunit, as noted for the apo protein.

Conclusions

The previously reported structure of apo calcyclin [9] revealed a unique homodimeric fold that appears to be conserved among all full-length S100 proteins and in the presence of Ca^{2+}. A subsequent analysis showed very substantial similarity between the structure of the apo calcyclin subunit and the apo state of the monomeric S100 protein, calbindin D_{9k}, particularly in the packing of their hydrophobic cores [28]. We have shown here that this structural homology extends to the Ca^{2+}-bound state of calcyclin.

There are only very small changes in the structure of the calcyclin subunit upon Ca^{2+} binding, similar to those observed in the case of calbindin D_{9k}. A detailed analysis of the Ca^{2+}-induced structural changes in calcyclin requires further refinement of both the apo and Ca^{2+}-bound structures, at a level corresponding to the high-resolution structures of calbindin D_{9k} [29,33,34]. The present structures, however, do provide a global view of the response to Ca^{2+} binding by the calcyclin homodimer. The changes are clearly very modest, similar to those observed for calbindin D_{9k}, but clearly different from the large Ca^{2+}-induced structural changes in the prototypical Ca^{2+} sensor calmodulin. Based on the high homology among S100 proteins, and the great similarity among the structures of apo and Ca^{2+}-bound calcyclin, apo and Ca^{2+}-bound calbindin D_{9k}, and apo S100β, we anticipate that all S100 proteins will undergo similar, small conformational changes upon binding Ca^{2+}.

The similarity of the three-dimensional structures of apo and Ca^{2+}-bound calcyclin contrasts sharply with the large structural changes (opening of the globular domains) of the prototypical Ca^{2+} sensors such as calmodulin and troponin C. The arrangement of the two globular domains in the calcyclin dimer is also clearly different from that of the two globular domains of calmodulin when free in solution or in complexes of calmodulin with target peptides [35]. This observation implies that calcyclin must have a distinct mode of receptor recognition. What then is the structural basis for the transduction of Ca^{2+} signals by calcyclin and other full-length S100 proteins? The Ca^{2+}-induced changes in calcyclin do not appear to be sufficient to trigger fundamental changes in protein–target interactions. If anything, the new structural information poses more questions than it provides answers.

Is it possible that S100 proteins are not actually Ca^{2+} sensors? While there is a considerable body of *in vitro* evidence to support the Ca^{2+}-dependent binding of S100 proteins to a variety of biological targets, there remains the nagging issue of Ca^{2+} affinities. The majority of S100

Figure 3

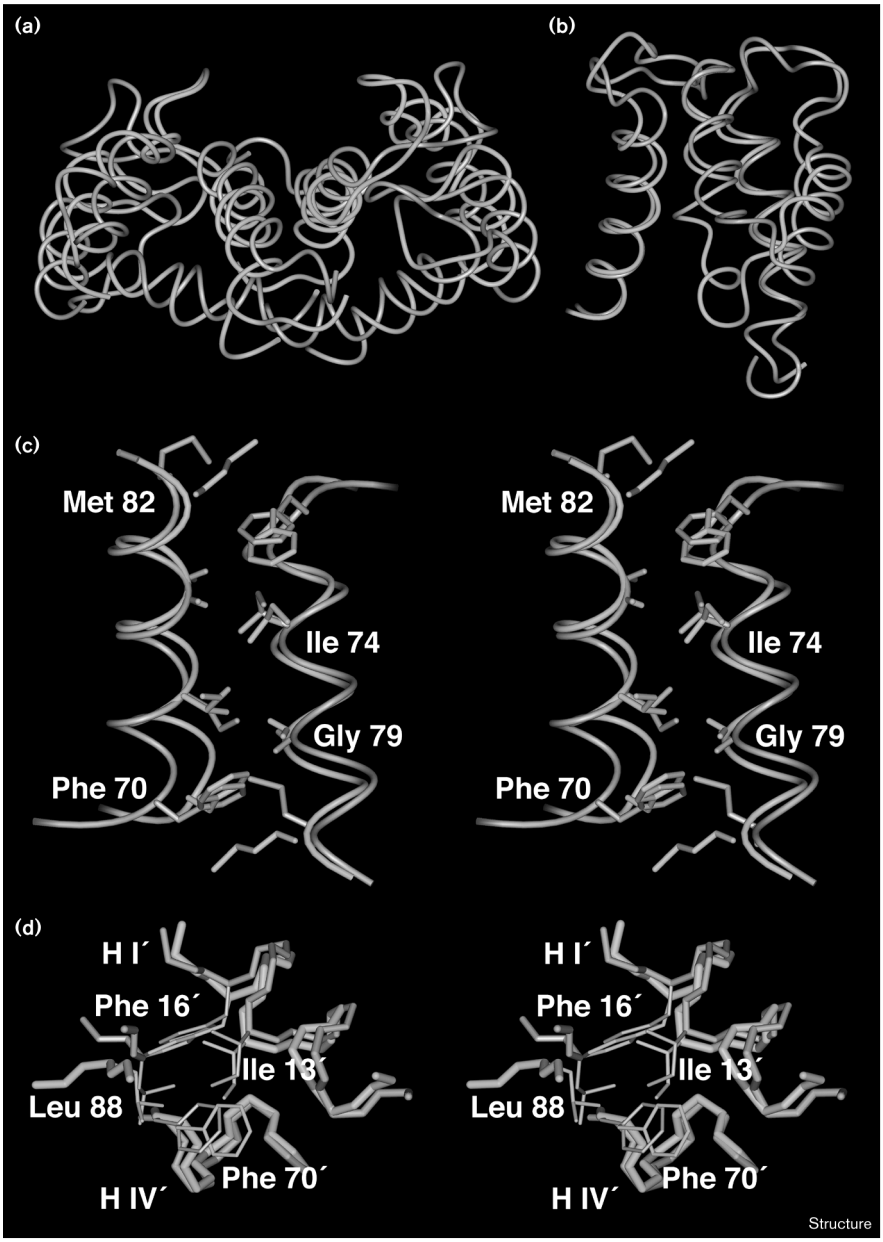

Comparison of the three-dimensional structures of calcyclin in the absence and presence of Ca^{2+}. **(a)** Overview of the representative apo (cyan) and Ca^{2+}-bound (salmon) structures displayed as smoothed Cα ribbons. **(b)** Overview of the similarity of the two structures at the level of the monomer, displayed as smoothed Cα ribbons. **(c)** Stereo close-up view from within the hydrophobic core of the helix IV–IV′ interface. **(d)** Stereo close-up view of the packing of the conserved hydrophobic residues Ile13′, Phe16′, Phe70′ and Leu88 at the dimer interface. The structures were overlaid in (a) and (b) by best-fit superposition of the backbone atoms of helices I, II and IV. The superposition in (c) was over all heavy atoms shown, and in (d) over the sidechain heavy atoms shown. The coordinates for apo calcyclin were obtained from the Brookhaven PDB (accession code 1CNP). (Figure prepared using Insight II [Version 95.0; MSI, San Diego].)

proteins bind Ca^{2+} with affinities in only the micromolar to millimolar range [12], for example the Ca^{2+} affinity of calcyclin is only 2.6×10^{-5} M in low ionic strength solutions (MS and WJC, unpublished results) and drops even lower at physiological ionic strength conditions [36]. Intracellular Ca^{2+} signaling is associated with 100-fold increases in Ca^{2+} concentration, generally accepted as occurring in the range ~10^{-7}–~10^{-5} M, which implies that most S100 proteins would not be able to respond to the Ca^{2+} signals. Ca^{2+} concentrations in the extracellular milieu are considerably higher, thus the purported extracellular Ca^{2+}-dependent activities assigned to S100 proteins are more readily explicable. Perhaps, in the intracellular milieu, the function of S100 proteins may be more intimately associated with properties that do not depend on Ca^{2+} binding, such as cell type specific and cell cycle dependent expression [12].

An alternative explanation for the low Ca^{2+} affinities would be that the biophysical data obtained *in vitro* do not accurately reflect the *in vivo* situation. Binding to targets could increase the affinity of S100 proteins for Ca^{2+}, conceivably raising the Ca^{2+}-binding constant into the range to be sensitive to intracellular Ca^{2+} signals. The

Table 3

Comparison of apo and Ca^{2+}-bound calcyclin.

	Backbone	All heavy atom
Dimer, helices* (Å)	1.9	2.3
Dimer, all (Å)	2.4	2.7
Subunit, helices* (Å)	1.2	1.7
Subunit, all (Å)	1.7	2.0

The table lists the root mean square deviations (rmsds) between the mean apo and the mean Ca^{2+}-bound structures. The mean subunit structure was calculated from the ensemble of 20 (Ca^{2+}-bound) or 22 (apo) dimer structures. The coordinates for apo calcyclin were obtained from the Brookhaven PDB (1CNP). *Helices are defined as: I, residues 5–20; II, 30–41; III, 50–61; and IV, 70–84.

binding to the target need not be of extremely high affinity, but of course would need to be 'productive' in the sense of potentiating Ca^{2+} binding. Although the absence of critical amino acids in the binding loops preclude Ca^{2+} binding by the S100 protein p11, its isolation as an integral component of the calpactin heterotetramer [37] provides supporting evidence for tight association with target proteins in the absence of Ca^{2+}. If pre-association is more common than anticipated *in vivo* and target binding induced increases in Ca^{2+} affinity are prevalent, this would rationalize the apparent anomaly between the reported binding constants *in vitro* and the *in vivo* function of S100 proteins in the direct readout of Ca^{2+} signals. The identification of target proteins *in vivo* and subsequent structural analysis of S100–target protein complexes are urgently needed to obtain deeper insight into the molecular basis of calcium-triggered cellular processes mediated by S100 proteins.

Biological implications

EF-hand calcium-binding proteins (CaBPs) play a central role in a variety of Ca^{2+} signaling pathways. Calcyclin is a member of the S100 subfamily of EF-hand CaBPs, which are characterized by N-terminal binding sites that are distinct from the EF-hand prototype. Calcyclin has been implicated in the regulation of cell growth and division, exhibits deregulated expression in association with cell transformation, and is found in high abundance in certain breast cancer cell lines.

The three-dimensional structure of apo calcyclin and subsequent structures of apo S100β revealed a novel homodimeric motif that is fundamentally different from that of the prototypical Ca^{2+} sensor calmodulin. These results implied that S100 proteins have a distinct mode of target recognition upon Ca^{2+} binding, which poses an interesting question: how are these dimeric structures triggered to interact with their receptor(s)? Herein we report the first step towards answering this question: the determination of the three-dimensional solution structure of Ca^{2+}-bound calcyclin.

The Ca^{2+}-bound state of calcyclin has a symmetric homodimeric fold similar to that of the apo protein. The dimer interface is mediated primarily by hydrophobic sidechain–sidechain interactions, as observed previously for apo calcyclin and apo S100β. Comparison of the currently available low- to medium-resolution structures in the absence and presence of Ca^{2+} provide a global view of the response to Ca^{2+} binding by the calcyclin homodimer. The Ca^{2+}-induced changes observed in calcyclin are rather modest, in stark contrast to the large structural changes seen in the classical Ca^{2+} sensors, such as calmodulin and troponin C. This observation suggests that calcyclin must have a subtle mode of receptor recognition, which is clearly distinct from that used by the classical Ca^{2+} sensors. The identification of target proteins and subsequent structural analysis of S100–target protein complexes will enhance our understanding of the molecular basis of cellular processes mediated by S100 proteins.

Materials and methods

NMR experiments

Recombinant rabbit calcyclin was over expressed in *Escherichia coli* (strain BL21[*DE3*]) containing a pET 1120 expression vector (derived from the pET 11 and pET 20 vectors from Novagen) with the calcyclin gene inserted. The samples enriched in ^{13}C and ^{15}N were produced by growth on M9 minimal media with $^{13}C_6$-glucose and $^{15}NH_4Cl$ as the sole carbon and nitrogen sources. The protein was purified by hydrophobic affinity perfusion chromatography on a BIOCAD Sprint System (Perceptive Biosystems). Three different samples were used to collect the NMR data, each at a concentration of 1–2 mM in 50 mM Tris-d_{11} buffer, 20–38 mM $CaCl_2$, and 0.04% w/v NaN_3, 95% H_2O–5% D_2O, at pH 7. One sample was uniformly enriched in ^{13}C (95%) and ^{15}N (99.8%), a second was enriched in ^{15}N only. The third sample used for the homonuclear ^1H experiments was not labeled. All NMR experiments were conducted at 27°C, using Bruker AMX-600, DRX-600 or DMX-750 spectrometers equipped with triple resonance probe heads and pulsed-field gradients. Spectra were processed and analyzed with FELIX software (version 95; MSI, San Diego).

Resonance assignments were obtained primarily using a combination of double and triple resonance experiments on the labeled samples [27]. The bulk of the backbone assignments were made from HNCA and HN(CO)CA spectra. These were confirmed and extended in CBCA(CO)NH, HNCACB, HNCO, HCACO, and ^{15}N TOCSY-HSQC spectra. Sidechain assignments were obtained primarily from HCCH-COSY and HCCH-TOCSY spectra. A 3D ^{15}N-^1H NOESY-HSQC-experiment ($\tau_m = 100$ ms) was thoroughly analyzed to assist in making the sequence-specific assignments for those residues that could not be readily assigned from the triple resonance spectra, due to multiple resonance degeneracies or poor S/N in the spectra.

Input data

The proton–proton distance constraints used in the structure calculations were obtained from a homonuclear ^1H NOESY spectrum ($\tau_m = 100$ ms), the 3D ^{15}N-^1H NOESY-HSQC ($\tau_m = 100$ ms), and a 3D ^{13}C-^1H NOESY-HSQC ($\tau_m = 80$ ms). The ^{15}N-^1H NOESY-HSQC provided all contacts between pairs of amide protons and the bulk of any other NOEs involving amides. The homonuclear ^1H NOESY was specifically analyzed to identify NOEs involving the aromatic and methyl proton resonances. The ^{13}C-^1H NOESY-HSQC was utilized primarily to differentiate between assignment possibilities for cross-peaks present in the two other spectra. This spectrum was analyzed

exhaustively only for a selected number of methyl groups. Upper bounds were set conservatively on the basis of cross-peak intensity. Constraints derived from the ^{1}H NOESY were given upper bounds of 4.0 Å, 5.0 Å and 6.0 Å, and from the ^{15}N NOESY-HSQC, 3.4 Å, 4.2 Å and 6.0 Å. All lower bounds were set to 1.8 Å. Pseudo-atom corrections were included where appropriate, as well as a 0.5 Å correction for motional averaging of all methyl groups, as described previously [38].

The NOE-derived distance constraints were supplemented by dihedral angle constraints and distance constraints for specifically identified hydrogen bonds. Helical and β-type ϕ and ψ constraints were assigned for 45 and six residues, respectively, on the basis of characteristic NOEs [39] and the chemical shift index [40] derived from C′, C^{α}, C^{β} and $C^{\alpha}H$ chemical shifts. Residues assigned to helical conformation by these criteria ($\phi = 60° \pm 20°$; $\psi = -40° \pm 40°$) included 5–19, 32–40, 50–60 and 70–83, which covers significant portions of each of the four helices in the protein. Dihedral angle constraints in extended conformation ($\phi = -120° \pm 25°$; $\psi = 120° \pm 50°$) were assigned for residues 28–30 and 67–69, corresponding to the characteristic cross-strand β-type interaction between the two Ca^{2+}-binding loops. Hydrogen bonds were assigned for 20 backbone amides exhibiting slow exchange with solvent and the NOEs characteristic of α-helical or antiparallel β-type conformation. For each hydrogen bond, the HN–O distance was constrained to 1.8–2.0 Å and the N–O distance to 2.7–3.0 Å.

Structure calculations

Structures were generated by a combination of distance geometry and rMD calculations, using the programs DISGEO [41] and AMBER (version 4.1) [42]. In the final round, 60 DISGEO calculations produced 27 converged subunit structures. These were minimized for 3000 steps using AMBER, then subjected to a standard 10 ps annealing cycle, as described elsewhere [9]. 48 dimer structures were created for each of the four best subunit structures using NAB [43; http://www.scripps.edu/case] to position two copies of the subunit 50 Å apart and systematically vary the relative orientation in 90° increments. These structures were docked by rMD over 20 ps, as described previously for apo calcyclin. The docked dimer structures were refined by 20 ps of rMD annealing. Of the 192 annealed structures, 136 could be discarded on the basis of high residual restraint violations and/or incorrect global fold. Calculations of average rmsd versus the number of structures for this ensemble using the program FindFam [44] showed that a minimum of 20 structures was required to represent the conformational space consistent with the available experimental data. The 56 converged structures were ordered by increasing experimental constraint violation energy and the 20 best were selected. Visual inspection of these 20 structures identified a subset of four structures as being 'out-of-family' in one or more regions of the molecule. Subsequent analysis of the dihedral and van der Waals' energy terms using the Anal module of AMBER on a per-residue basis revealed that certain values exceeded twice the standard deviation from the mean value in these out-of-family regions [38]. Consequently, the four aberrant structures were replaced by the next four from the full ensemble. The single structure selected to represent the ensemble is that closest to the geometric mean.

Structure analyses

PROCHECK NMR software [45] was used to examine the structural features of the final ensemble. Interhelical angles were measured using software provided by SM Gagné (University of Alberta, Edmonton). Distance difference matrices and interresidue contact analyses were calculated as described elsewhere [32]. Molecular graphics analysis and parameter visualization was carried out using Insight II (Version 95.0; MSI, San Diego).

Accession numbers

The coordinates for the final ensemble of 20 structures along with the input constraint lists have been deposited at the Protein Data Bank with accession number 1A03.

Acknowledgements

We thank Garry Gippert for providing GENXPK and GAP software tools to assist in assigning NOE cross-peaks, Jarrod A Smith for assistance with the structure calculations, Melanie R Nelson for software to analyze distance difference matrices and interresidue contacts, and JAS, GG, MRN, Lena Mäler, David Weber and Gary Shaw for helpful discussions. This research was supported by the National Institutes of Health (PO1 GM-48495) and the Monbusho International Science Research Program. WJC is a Faculty Research Fellow of the American Cancer Society.

References

1. Kuboniwa, H., Tijandra, N., Grzesiek, S., Ren, H., Klee, C.B. & Bax, A. (1995). Solution structure of calcium-free calmodulin. *Nat. Struct. Biol.* **2**, 768-776.
2. Zhang, M., Tanaka, T. & Ikura, M. (1995). Calcium-induced conformational transition revealed by the solution structure of apo calmodulin. *Nat. Struct. Biol.* **2**, 758-767.
3. Finn, B.E., Evenäs, J., Drakenberg, T., Waltho, J.P., Thulin, E. & Forsén, S. (1995). Calcium-induced structural changes and domain autonomy in calmodulin. *Nat. Struct. Biol.* **2**, 777-783.
4. Gagné, S.M., Tsuda, S., Li, M.X., Smillie, L.B. & Sykes, B.D. (1995). Structures of the troponin C regulatory domains in the apo and calcium-saturated states. *Nat. Struct. Biol.* **2**, 784-789.
5. Herzberg, O., Moult, J. & James, M.N.G. (1986). A model for the Ca^{2+}-induced conformational transition of troponin C. *J. Biol. Chem.* **261**, 2638-2644.
6. Ikura, M., Clore, G.M., Gronenborn, A.M., Zhu, G., Klee, C.B. & Bax, A. (1992). Solution structure of a calmodulin-target peptide complex by multidimensional NMR. *Science* **256**, 632-638.
7. Meador, W.E., Means, A.R. & Quiocho, F.A. (1992). Target enzyme recognition by calmodulin: 2.4 Å structure of a calmodulin–peptide complex. *Science* **257**, 1251-1255.
8. Meador, W.E., Means, A.R. & Quiocho, F.A. (1993). Modulation of calmodulin plasticity in molecular recognition on the basis of X-ray structures. *Science* **262**, 1718-1721.
9. Potts, B.C.M., *et al.*, & Chazin, W.J. (1995). The structure of calcyclin reveals a novel homodimeric fold for S100 Ca^{2+}-binding proteins. *Nat. Struct. Biol.* **2**, 790-796.
10. Kilby, P.M., van Eldik, L.J. & Roberts, G.C.K. (1996). The solution structure of the S100β protein dimer in the calcium-free state. *Structure* **4**, 1041-1051.
11. Drohat, A.C., Amburgey, J.C., Abildgaard, F., Starich, M.R., Baldisseri, D. & Weber, D.J. (1996). Solution structure of Rat apo-S100B(ββ) as determined by NMR spectroscopy. *Biochemistry* **35**, 11577-11588.
12. Schäfer, B.W. & Heizmann, C.W. (1996). The S100 family of EF-hand calcium-binding proteins: functions and pathology. *Trends Biochem. Sci.* **21**, 134-140.
13. Strynadka, N.C.J. & James, M.N.G. (1989). Crystal structures of the helix-loop-helix calcium-binding proteins. *Annu. Rev. Biochem.* **58**, 951-998.
14. Calabretta, B., *et al.,* & Baserga, R. (1985). Cell-cycle-specific genes differentially expressed in human leukemias. *Proc. Natl. Acad. Sci. USA* **82**, 4463-4467.
15. Hirschhorn, R.R., Aller, P., Yuan, Z.-A., Gibson, C.W. & Baserga, R. (1984). Cell-cycle-specific cDNAs from mammalian cells temperature sensitive for growth. *Proc. Natl. Acad. Sci. USA* **81**, 6004-6008.
16. Ferrari, S., *et al.*, Baserga, R. (1987). Structural and functional analysis of a growth-regulated gene, the human calcyclin. *J. Biol. Chem.* **262**, 8325-8332.
17. Schäfer, B.W., Wicki, R., Engelkamp, D., Mattei, M.-G. & Heizmann, C.W. (1995). Isolation of a YAC clone covering a cluster of nine S100 genes on human chromosome 1q21: rationale for a new nomenclature of the S100 calcium-binding protein family. *Genomics* **25**, 638-643.
18. Calabretta, B., *et al.*, Baserga, R. (1986). Altered expression of G_1-specific genes in human malignant myeloid cells. *Proc. Natl. Acad. Sci. USA* **83**, 1495-1498.
19. Murphy, L.C., Murphy, L.J., Tsuyuki, D., Duckworth, M.L. & Shiu, R.P.C. (1988). Cloning and characterization of a cDNA encoding a highly conserved, putative calcium binding protein, identified by an anti-prolactin receptor antiserum. *J. Biol. Chem.* **263**, 2397-2401.
20. Minami, H., Tokumitsu, H., Mizutani, A., Watanabe, Y., Watanabe, M. & Hidaka, H. (1992). Specific binding of CAP-50 to calcyclin. *FEBS Lett.* **305**, 217-219.

21. Watanabe, M., Ando, Y., Tokumitsu, H. & Hidaka, H. (1993). Binding site of annexin XI on the calcyclin molecule. *Biochem. Biophys. Res. Commun.* **196**, 1376-1382.
22. Zeng, F.-Y., Gerke, V. & Gabius, H.-J. (1993). Identification of annexin II, annexin VI and glyceraldehyde-3-phosphate dehydrogenase as calcyclin-binding protein in bovine heart. *Int. J. Biochem.* **25**, 1019-1027.
23. Filipek, A. & Kuznicki, J. (1998). Molecular cloning and expression of a mouse brain cDNA encoding a novel protein target of calcyclin. *J. Neurochem.*, in press.
24. Tokumitsu, H., Mizutani, A., Minami, H., Kobayashi, R. & Hidaka, H. (1992). A calcyclin-associated protein is a newly identified member of the Ca^{2+}/phospholipid binding proteins, annexin family. *J. Biol. Chem.* **267**, 8919-8924.
25. Tokumitsu, H., Mizutani, A. & Hidaka, H. (1993). Calcyclin-binding site located on the NH_2-terminal domain of rabbit CAP-50 (annexin XI): functional expression of CAP-50 in *Escherichia coli*. *Arch. Biochem. Biophys.* **303**, 302-306.
26. Mizutani, A., *et al.*, Hidaka, H. (1992). CAP-50, a newly identified annexin, localizes in nuclei of cultured fibroblast 3Y1 cells. *J. Biol. Chem.* **267**, 13498-13504.
27. Cavanagh, J., Fairbrother, W.J., Palmer, A.G. III. & Skelton, N.J. (1996). *Protein NMR Spectroscopy, Principles and Practices.* Academic Press, Inc. San Diego, CA.
28. Potts, B.C.M., Carlström, G., Okazaki, K., Hidaka, H. & Chazin, W.J. (1996). ^1H NMR assignments of apo calcyclin and comparative structural analysis with calbindin D_{9k} and S100β. *Protein Sci.* **5**, 2162-2174.
29. Kördel, J., Pearlman, D.A. & Chazin, W.J. (1997). Protein solution structure calculations in solution: solvated molecular dynamics refinement of calbindin D_{9k}. *J. Biomol. NMR* **10**, 231-243.
30. McPhalen, C.A., Strynadka, N.C. & James, M.N. (1991). Calcium-binding sites in proteins: a structural perspective. *Adv. Protein Chem.* **42**, 77-144.
31. Skelton, N.J., Kördel, J., Akke, M., Forsén, S. & Chazin, W.J. (1994). Signal transduction versus buffering activity in Ca^{2+}- binding proteins. *Nat. Struct. Biol.* **1**, 239-245.
32. Nelson, M. & Chazin, W. (1998). An interaction-based analysis of calcium-induced conformational changes in Ca^{2+}-sensor proteins. *Protein Sci.* **7**, 270-282.
33. Skelton, N.J., Kördel, J. & Chazin, W.J. (1995). Determination of the solution structure of apo calbindin D_{9k} by NMR spectroscopy. *J. Mol. Biol.* **249**, 441-462.
34. Kördel, J., Skelton, N.J., Akke, M. & Chazin, W.J. (1993). High-resolution solution structure of calcium-loaded calbindin D_{9k}. *J. Mol. Biol.* **231**, 711-734.
35. Crivici, A. & Ikura, M. (1995). Molecular and structural basis of target recognition by calmodulin. *Annu. Rev. Biophys. Biomol. Struct.* **24**, 85-116.
36. Pedrocchi, M., Schäfer, B.W., Durussel, I., Cox, J.A. & Heizmann, C.W. (1994). Purification and characterization of the recombinant human calcium-binding S100 proteins CAPL and CACY. *Biochemistry* **33**, 6732-6738.
37. Weber, K. (1992). Annexin II: interaction with p11. In *The Annexins*. (Moss, S.E. ed), pp. 61-68, Portland press, London.
38. Akke, M., Forsén, S. & Chazin, W.J. (1995). Solution structure of $(Cd^{2+})_1$-calbindin D_{9k} reveals details of the stepwise structural changes along apo$\rightarrow(Ca^{2+})_1^{II}\rightarrow(Ca^{2+})_2^{I,II}$ binding pathway. *J. Mol. Biol.* **252**, 102-121.
39. Wüthrich, K. (1989). Protein structure determination in solution by nuclear magnetic resonance spectroscopy. *Science* **243**, 45-50.
40. Wishart, D.S., Sykes, B.D. & Richards, F.M. (1992). The chemical shift index: a fast and simple method for the assignment of protein secondary structure through NMR spectroscopy. *Biochemistry* **31**, 1647-1651.
41. Havel, T. & Wüthrich, K. (1984). A distance geometry program for determining the structures of small proteins and other macromolecules from nuclear magnetic resonance measurements of intramolecular ^1H-^1H proximities in solution. *Bull. Math. Biol.* **46**, 673-698.
42. Pearlman, D.A., *et al.*, Kollman, P.A. Amber 4.1. University of California, San Francisco.
43. Macke, T.J. (1996). NAB: a language for molecular manipulation. PhD thesis, The Scripps Research Institute, La Jolla, CA, USA.
44. Smith, J.A., Gomez-Paloma, L., Case, D.A. & Chazin, W.J. (1996). Molecular dynamics docking driven by NMR-derived restraints to determine the structure of the calicheamicin γ_1^1 oligosaccharide domain complexed to duplex DNA. *Magn. Reson. Chem.* **34**, S147-S155.
45. Laskowski, R.A., MacArthur, M.W., Moss, D.S. & Thornton, J.M. (1993). PROCHECK: a program to check the stereochemical quality of protein structures. *J. Appl. Cryst.* **26**, 283-291.
46. Carsen, M. (1991). Ribbons 2.0. *J. Appl. Cryst.* **24**, 958-961.